International Journal in Physical and Applied Sciences
Volume 06 Issue 12, December 2019 ISSN: 2394-5710 Impact Factor: 4.657
Journal Homepage: http://ijmr.net.in, Email: irjmss@gmail.com
Double-Blind Peer Reviewed Refereed Open Access International Journal

INFLUENCES OF THE SHAPE OF SPECIMEN WITH CENTRAL CRACK FOR BIAXIAL TENSILE LOADING ON THE STRESS FIELDS NEAR THE CRACK-TIP

Dong-Chul Shin
Department of Mechanical Engineering, Koje College, Geoje, Gyeongnam, 53325, Korea

Abstract:
Hybrid method for photoelasticity is here introduced and used to study on the fracture problems of central cracked cruciform specimens with or without slots in its arms under equal biaxial tensile loading. And actual isochromatics, stress components and stress intensity factors in the vicinity of crack tip with the two type biaxial loading specimen were compared. From the results, we recognized that the specimen with slots in the arms is more effective to make equal biaxial stress state than the specimen without slot, and found that the distribution shape of stress components in the vicinity of crack-tip are similar to each other, but the magnitude of stress components and stress intensity factors in the specimen without slot are higher than those in the specimen with slots in the arms.

Keywords: *Biaxial Tensile Loading, Cruciform Specimen, Hybrid Method for Photoelasticity, Mixed Mode Crack, Stress Fields, Stress Intensity Factors.*

Introduction

Almost structural and machine components are under rarely uniaxial loading, but biaxial or multiaxial loading. Therefore, it is important to study and evaluate biaxial effects in order to improve prediction capability of crack propagation for design more realistic structure and machine parts. According to the previous works, the solutions using purely elastic formulations for fracture problems involving crack were not theoretically affected by the lateral stress component (Miler and Kfouri, 1974), but, in actual, biaxial stresses affect the behaviors such as the direction of crack propagation (Jones and Eftis, 1981) and the fatigue crack growth rate (Yu *et al*.,2002). Therefore, the experimental studies on the fracture behaviors under various biaxial loading conditions must be carried out because these conditions are more actual stress state rather than uniaxial loading condition.

For studies on the biaxial loading, Swanson *et al*. (1986, 1992) found that there is little interaction between longitudinal loading and transverse loading in tubular specimens when matrix-dominated modes are restrained. Lim *et al*. (2001) theoretically studied the biaxial load effects on crack extension in anisotropic solids using the maximum circumferential tensile stress criterion. Shimamoto *et al*. (2000) calculated the stress intensity factors in central cracked cruciform specimens of elastic and anisotropic material under various biaxial load ratios by the photoelastic and caustic experimental methods. Liu *et al*. (1979) suggested the criteria for designing configuration of biaxial loading specimen. And then, in this study, we designed a biaxial loading specimen based on the Liu's criteria as shown in figure 1 (b), and verified its validity using by finite element analyses and photoelastic experiments.

In order to analyses the photoelastic experiment results, the hybrid method for photoelasticity was used in this research. The hybrid method for photoelasticity was firstly introduced by Hawong *et al*. (1995), and Shin *et al*. (1998, 2001, 2016) widely used to study on the stress fields and stress intensity factors (SIFs) near the crack-tip in elastic materials and orthotropic materials. However, there were little research for studying influences of equal biaxial tensile loads on the isochromatic fringes, stress fields and stress intensity factors near the crack tip using the hybrid method for photoelasticity.

Thus, this work will be carried out a study of these phenomena using the hybrid method for photoelasticity. In other words, this research is focusing on verifying the superiority of our new designed specimen with slots comparison with the conventional specimen without slots by using finite element analysis, photoelastic experiments and hybrid method for photoelasticity.

Stress Fields Near Crack-tip and Hybrid Method for Photoelasticity

Stress components of plane problem in the isotropic material can be expressed by the power series as follows (Shin *et al.*, 1998)

$$\begin{aligned}
\sigma_x &= \sum_{n=1}^{N} \mathbf{Re}\left\{C_n\left[2f(n,z) - g(n,z)\right] + (-1)^n \overline{C_n} f(n,z)\right\} \\
\sigma_y &= \sum_{n=1}^{N} \mathbf{Re}\left\{C_n\left[2f(n,z) + g(n,z)\right] - (-1)^n \overline{C_n} f(n,z)\right\} \qquad (1) \\
\tau_{xy} &= \sum_{n=1}^{N} \mathbf{Im}\left\{C_n g(n,z) - (-1)^n \overline{C_n} f(n,z)\right\}
\end{aligned}$$

$$\text{where } f(n,z) = \frac{n}{2} z^{\frac{n}{2}-1}, \quad g(n,z) = \frac{n}{2}\left\{\bar{z}\left(\frac{n}{2}-1\right) - \frac{n}{2} z\right\} z^{\frac{n}{2}-2}, \quad z = x + iy$$

For applying to photoelastic experiment, substituting equation (1) into the stress optic law (Sampson, 1970) gives

$$\begin{aligned}
\left(\frac{f \cdot N_f}{t}\right)^2 &= \left(\sigma_x - \sigma_y\right)^2 + \left(2\tau_{xy}\right)^2 \\
&= \left\{2\sum_{n=1}^{N} a_n \mathbf{Re}\left[f_c(n,z) - g_c(n,z)\right] + 2\sum_{n=1}^{N} b_n \mathbf{Im}\left[f_c(n,z) + g_c(n,z)\right]\right\}^2 \qquad (2) \\
&+ \left\{2\sum_{n=1}^{N} a_n \mathbf{Im}\left[g_c(n,z) - f_c(n,z)\right] + 2\sum_{n=1}^{N} b_n \mathbf{Re}\left[f_c(n,z) + g_c(n,z)\right]\right\}^2
\end{aligned}$$

$$\text{where } f_c(n,z) = (-1)^n f(n,z), \quad g_c(n,z) = g(n,z)$$

Here f is stress fringe value of specimen, t is the thickness of specimen, z is the position from the crack-tip, and N_f is the isochromatic fringe order at the position z. Therefore, the complex coefficients $C_n = a_n + ib_n$ are only unknown quantities in equation (2). a_n and b_n can be calculated by the nonlinear least squares method for the photoelastic experiment (Shin *et al.*, 1998, 2001). And then, the stress components near the crack-tip can be obtained by substituting the calculated C_n into equation (1). This process is well known as the hybrid method for photoelasticity for fracture problem of the linear elastic isotropic material.

The relationships between the stress intensity factors and the complex coefficients C_n are given in equation (3) (Shin *et al.*, 1998)

$$K_0 = \sigma_0 \sqrt{\pi a}, \quad K_I = \sqrt{2\pi} a_1, \quad K_{II} = \sqrt{2\pi} b_1 \qquad (3)$$

where σ_0 is far-field stress applied to the specimen, a is half of the crack length and $C_1 \left(= a_1 + ib_1\right)$ is the complex coefficient when *n*=1 at the Eq. (2).

Experiment and Experimental Method

Specimen Configuration and photoelastic experiment system

Liu et al. (1979) suggested the criteria for designing a biaxial specimen configuration, the criterial are mainly as follows:

1) The size of the specimen should be large enough to minimize boundary effects on crack tip stress intensity factor; but it should not be too large, so that the required load levels can be kept within the capacity of the testing machine.
2) The stress distribution across the specimen width should be fairly uniform

So, we prepared a new improved biaxial specimen with slots in their arms as shown in figure 1 (b). Figure 1 (a) is conventional specimen which is widely used in the biaxial loading test so far. As shown in figure 1, the shapes and dimensions of the specimens without slots and with slots can be observed, and the coordinate system (X,Y) and (x,y) are taken as shown in the figures. The two type specimens have equally overall length of 300 mm including grip areas at each end of the loading arms.

The photoelastic specimens were poly-carbonate plate (PS1S, Measurements Group, Inc) which is an isotropic material, and its physical properties are that f=6.993 kN/m, Young's modulus E=2.5 GPa and Poisson's ratio $\nu = 0.38$. Height and width of all specimen are 300 mm, but the thickness (t) and width of specimen arms (w) of two type specimens are different each other, that is, t=3 mm and w= 140 mm in case of specimen with slots and , t=6 mm and w= 60 mm in case of specimen without slots. A central crack with an inclined angle, $\beta = 0^{o}$ and 45^{o} was machined to 28 mm length by the long end mill of the 0.8mm diameter, and then the crack-tip was manufactured by a razor edge of 0.08mm thickness to sharpen natural crack more to 1mm in both sides of the crack-tip until the total length of crack ($2a$) is 30 mm.

For this research, the photoelastic experimental system with hydraulic type biaxial loading device was used as shown in figure 2. The device can control various biaxial load ratios between X-Y axes under biaxial loading condition since the two axes are independent each other. The photographs of isochromatic fringe pattern had been taken by CCD camera system (FASTCAM-Net 500C/1000C/ Max: PHOTRON).

Figure 1. Dimensions of cruciform specimens (Unit: mm)

(a) Specimen without slot (b) Specimen with slots

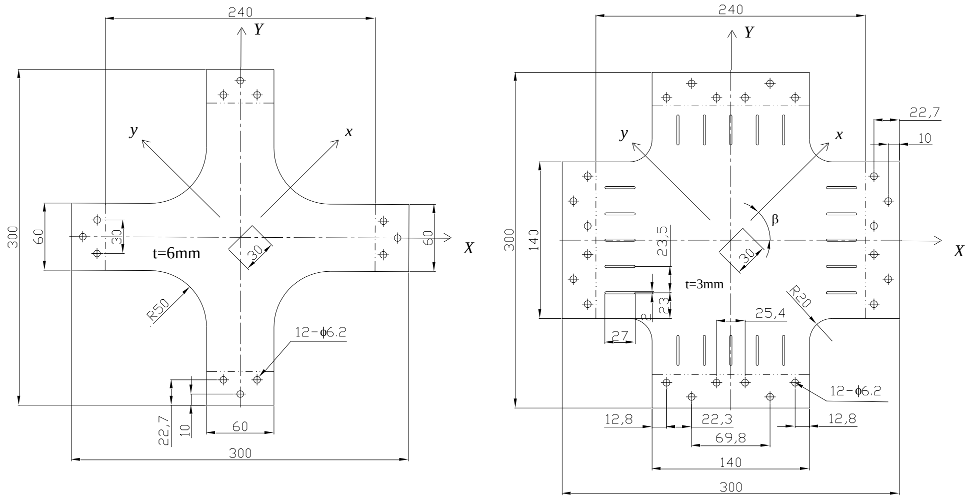

Figure 2. Photoelastic experiment system with biaxial loading device

Experimetal results and discussion

In order to verifying of two specimens, finite element analyses for rectangular plates with central crack under the uniform biaxial stress state ($\alpha = \sigma_X / \sigma_Y = 1$)were performed, and then the isochromatic fringe patterns were regenerated from the result data obtained by the finite element analyses as shown in figure 3. In finite element analyses, the two-dimensional isoparametric element with eight nodes was used, and sufficiently fine mesh was employed to generate the isochromatic fringe patterns obtained from the stress components around crack tip.

Figure 3. Isochromatics of idealized square specimen under the equal biaxial stress (α =1) loading obtained from finite element analysis

(a) (β =0°, α =1) (b) (β =45°, α =1)

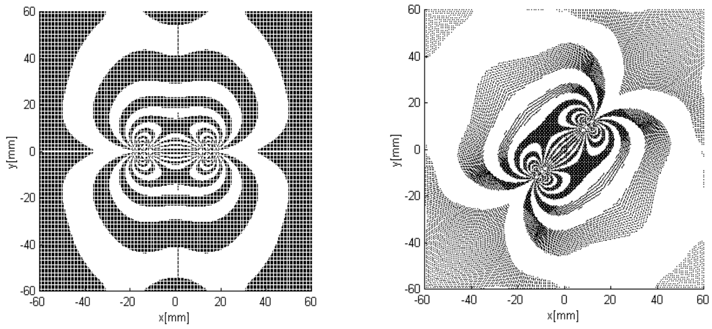

Figure 4. Actual isochromatics in the cruciform specimens under equal biaxial loading (γ =1)

Specimens without slot in the arms Specimens with slots in the arms

(a) β =0° (b) β =45° (c) β =0° (d) β =45°

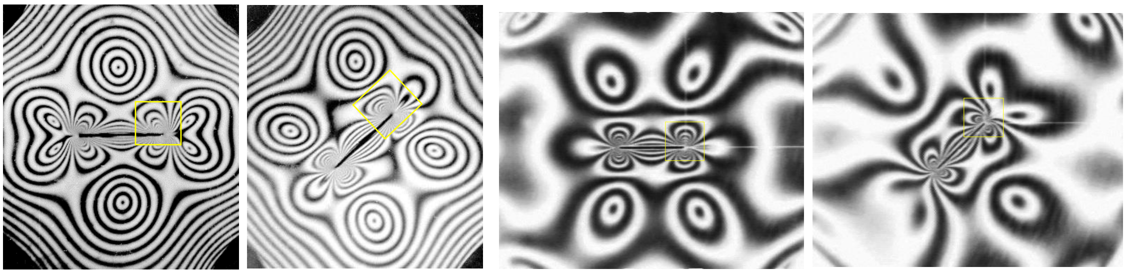

For comparing two specimens, photoelastic experiments also were carried out by using the developed biaxial loading device and the results are represented in figure 4. The biaxial tensile loads (P_X and P_Y) of 400 kgf were applied to the improved specimen with slots, and 300kgf to the conventional specimen without slot in both (*X* and *Y*) directions, that is, biaxial load ratios ($\gamma = P_X / P_Y$) are 1. It should note that the (*X*, *Y*) is a Cartesian coordinate system in which the *X* -axis is parallel to the direction of the horizontal arms of the biaxial specimen and the origin is the central point of specimen, but the (*x*, *y*) is a coordinate system where the x-axis coincides with the line of crack and the origin is the crack tip, as shown in figure 1.

As is seen in figure 4, the isochromatic fringe patterns of both specimens very near crack are similar to each other and also similar to those of figure. 3, thus both specimens were verified as the biaxial tensile loading specimen. However the isochromatics at distance from crack are very difference between two type specimens, and the isochromatics far from crack in both specimens are contrary to each other, that is, the isochromatics of horizontal crack (45^{o} inclined

Figure 5. Actual and regenerated isochromatics for biaxial loading specimen without slot

(a) β =0° (b) β =45°

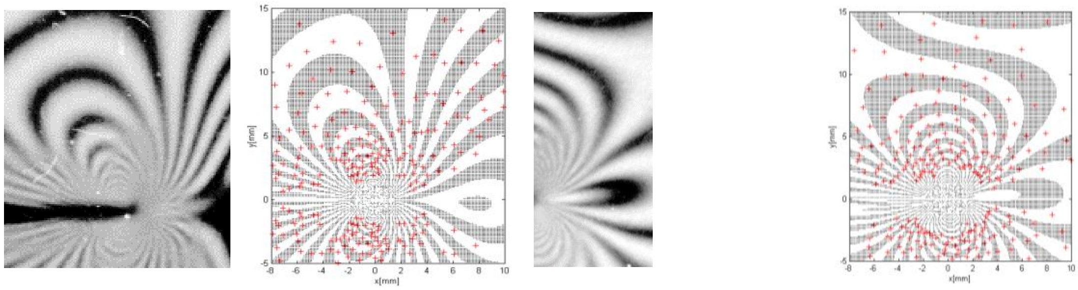

Figure 6. Contour plots of normalized stress components in the vicinity of the crack-tip of biaxial loading specimen without slot under equal biaxial loading (γ =1)

σ_x / σ_0 σ_y / σ_0 τ_{xy} / σ_0

(a) β =0°

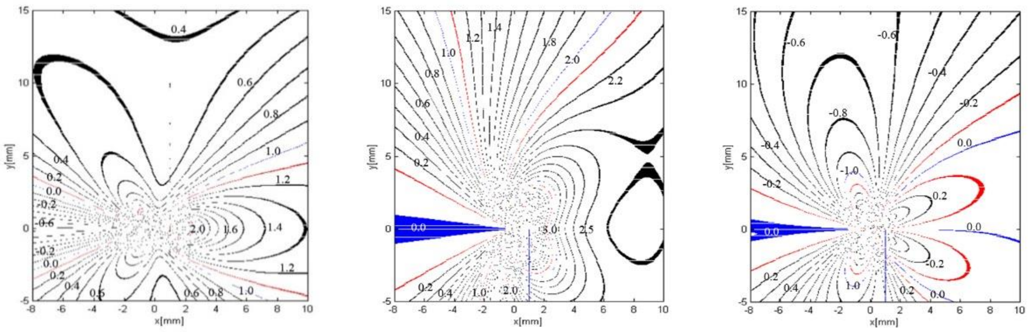

(b) β =45°

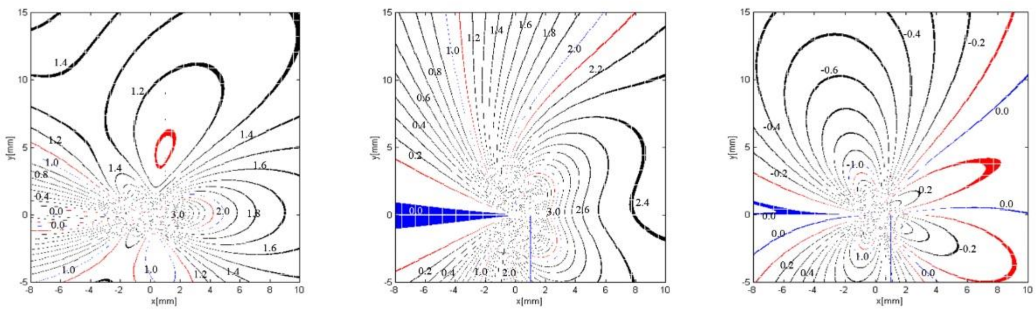

crack) of the specimen without slot in the arms are similar to those of 45° inclined crack (horizontal crack) of specimen with slots. Form comparing figure 3 with figure 4, it can be also found that those of improved specimen with slots is more similar to those of idealized specimens in the figure 3, and observed that the gradient of isochromatics in the outer boundary region in figure 4 (c) and (d) are less intense than those of figure 4 (a) and (b). Therefore, the specimen with slots is more effective to make biaxial stress uniform than without slot.

Figures 5 and 7 show that the actual isochromatics (ones in the rectangular boxes "□" in the figures 4(a)~(d)) and the regenerated ones calculated from the obtained stress components through the hybrid method for photoelasticity when the biaxial tensile load (γ =1) were applied to the two type biaxial specimens with a central crack of inclined angle, β =0° and 45°.

Figure 7. Actual and regenerated isochromatics for biaxial loading specimen with slots

(a) β =0° (b) β =45°

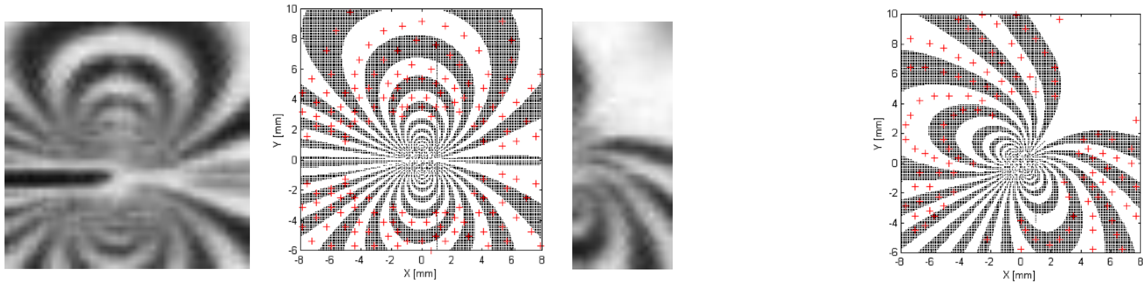

Figure 8. Contour plots of normalized stress components in the vicinity of the crack-tip of biaxial loading specimen with slots under equal biaxial loading (γ =1)

σ_x / σ_0 σ_y / σ_0 τ_{xy} / σ_0

(a) β =0°

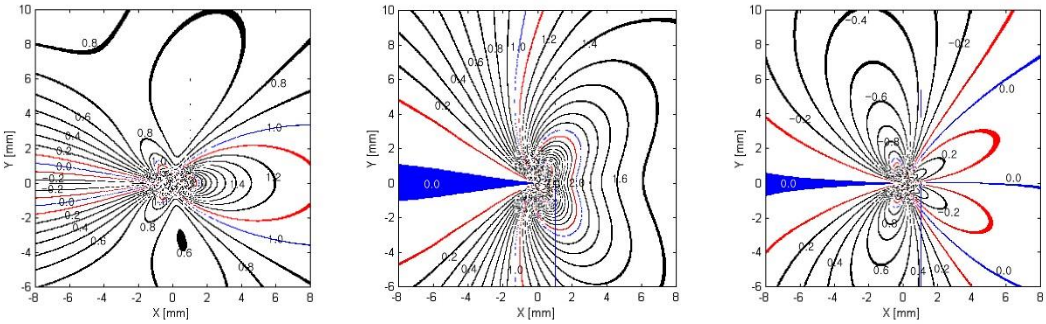

(b) β =45°

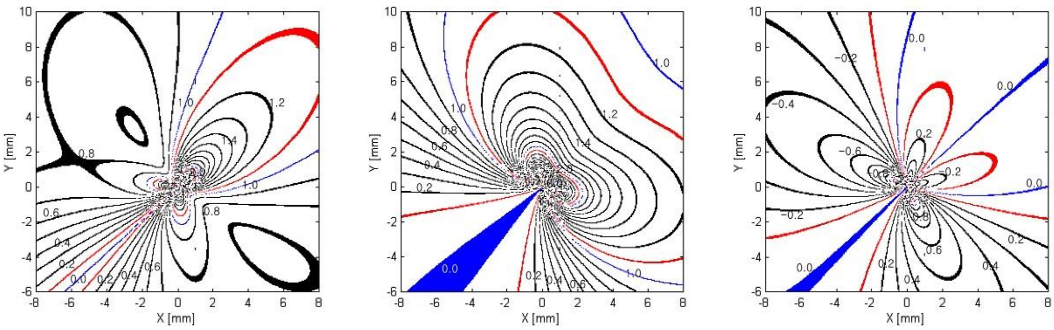

The isochromatic fringe data were measured on the center of each fringe band which are x.0 (black) or x.5 (white) fringe orders and marked by "+". As shown in figures 5 and 7, the regenerated isochromatic fringes are almost identical to the actual ones and "+" marks are located at the center of isochromatic bands. Thus, it can be verified that the hybrid method for photoelasticity used in this research is effective.

Figures 6 and 8 show contours of the normalized stress components (σ_x / σ_0, σ_y / σ_0 and τ_{xy} / σ_0) in the vicinity of the crack tip obtained by using the coefficients determined from the hybrid method for photoelasticity in the figures 5 and 7, respectively. All stress components were normalized by the applied far-field stress ($\sigma_0 = P_Y/(w \cdot t)$), and the contour lines have been increased by 0.1 steps. It should be noted that the X-axis is parallel to the horizontal line and the crack tip is the origin in the Cartesian coordinate system (*X*, *Y*) as is mentioned above, and all stress components were calculated with respect to the Cartesian coordinate system (*x*, *y*). In the figures 6 and 8, it can be seen that the values of σ_y and τ_{xy} on the crack surface are zero, and thus the traction free condition on the crack surface is satisfied. Comparing with the shapes and orders of contour lines of stress components in the figures 6 and 8, it can be found that, regardless of the inclined angle of crack, the distributions of all stresses are symmetric about the line of crack (that is in the Mode I condition) and the distribution shapes are very similar to each case. And the shapes and orders of contour lines of stress components in case of β=45^o are also very similar and equal to those in case of β=0 ^{o}, irrespective to the existence of slots. But the magnitudes of all the normalized stress components near the crack-tip in the specimen without slot are only higher than those in the specimen with slots.

Figure 9 represents the normalized stress intensity factors (SIF's) for each case of figures 6 and 8. The SIF's were calculated by using equation (3) and the complex coefficients obtained from the hybrid method for photoelasticity, and normalized by $K_0 (= \sigma_0 \sqrt{\pi a})$. As shown in figure 9, the values of K_{II}/K_0 are almost zero that means the all cases are Mode I condition under the biaxial loading when the inclined angle of crack β=0 ^{o} and 45^o, and the values of K_I/K_0 are a little decreased as the inclined angle of crack increases. In addition, the values of K_I/K_0 in the specimens without slot are all higher than those in the specimen with slots in the loading arms, these are similar to the magnitude of stress components at the crack-tip.

Figure 6. Normalized stress intensity factors with the inclined angle of crack

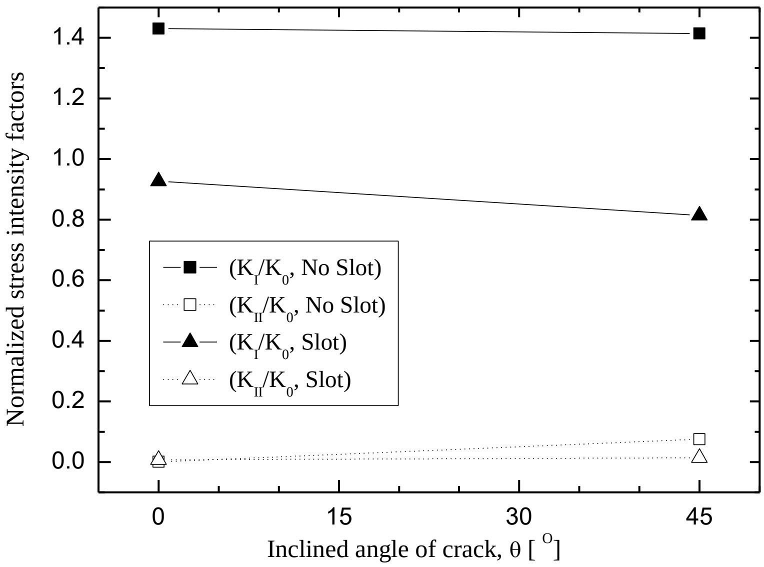

Conclusions

The following conclusions were obtained through the study on the influences of the shape of biaxial central cracked specimen (that is, the existence of slots in the arms) on the variation of isochromatics, stress fields and stress intensity factors in the vicinity of crack tip under the equal biaxial tensile loading.

1. Validity of the hybrid method for photoelasticity used for the biaxial tensile loading test was verified in this research.

2. As the equal biaxial load is subjected to the specimen with/without slots, regardless of the inclined angle of crack, the isochromatic fringe loops were symmetric about the line of crack, i.e. mode I condition.

3. Comparing with idealized equal biaxial stress state, the isochromatic fringe patterns in the specimen with slots in the arms are more similar to ones in the idealized specimen than ones in the specimen without slot. That means the specimen with slots is more effective to make biaxial stress uniform than the specimen without slot.

4. Regardless of the inclined angle of crack, the distributions of all stresses are symmetric about the line of crack and the distribution shapes are very similar to each case. But the magnitudes of all the normalized stress components near the crack-tip in the specimen without slot are only higher than those in the specimen with slots.

5. Irrespective to the existence of slots, the shapes and orders of contour lines of stress components in case of $\beta = 45^o$ are also very similar and equal to those in case of $\beta = 0^o$.

6. The values of K_{II}/K_0 in two specimen with/without slots are almost zero under equal biaxial loading when the inclined angle of crack $\beta = 0^o$ and 45^o, this means the all cases are Mode I condition. In addition, the values of K_I/K_0 in the specimens without slot are all higher than those in the specimen with slots in the loading arms

References

K.J. Miler and A.P. Kfouri (1974), An elastic-plastic finite element analysis of crack tip fields under biaxial loading conditions, *International Journal of Fracture*, **10(3)**, 393-404.

D.L. Jones and J. Eftis (1980), Fracture and Fatigue Characterization of Aircraft Structural Materials Under Biaxial Loading. Final Scientific Report. *AFOSR*, Washington, D.C.

Y. Yu, M. Wan, X.D. Wu and X.B. Zhou (2002), Design of a cruciform biaxial tensile specimen for limit strain analysis by FEM, J. of Materals Processing Technology, **123**, 67-70.

S. R. Swanson and A. P. Christoforou (1986), Response of Quasi-Isotropic Carbon/Epoxy Laminates to Biaxial Stress, *Journal of Composite Materials*, **20**, 457-471.

S. R. Swanson (1992), Biaxial Failure Criteria for Toughened Resin Carbon/Epoxy laminates, *Proceedings of the American Society for Composites 7th Technical Conference* 1075-1083.

Won-Kyun Lim, Seung-Yong Choi and Bhavani V. Sankar (2001), Biaxial Load Effects on Crack Extension in Anisotropic Solids, *Engineering Fracture Mechanics*, **68**, 403-416.

A. Shimamoto, J. H. Nam, T. Shimomura, and E. Umezaki (2000), Determination of SIF in isotropic and anisotropic body by the Photoelastic and Caustics Methods under Various Load Ratios, *Key Engineering Materials*, **183-187**, 115-120.

A. Liu, J. Allison, D. Dittmer, and J. Yamane (1979), "Effect of Biaxial Stresses on Crack Growth," in Fracture Mechanics: Proceedings of the Eleventh National Symposium on Fracture Mechanics: Part I, ed. C. Smith (West Conshohocken, PA: ASTM STP 677), 5-22.

J. S. Hawong, C. H. Lin, S. T. Lin, J. Rhee and R. E. Rowlands (1995), A Hybrid method to Determine Individual Stresses in Orthotropic Composites Using Only Measured Isochromatic Data, Joural of Compsite Material, **29(18)**, 2366-2387.

D. C. Shin, J. S. Hawong, H. J. Lee, J. H. Nam and O. S. Kwon (1998), Application of Transparant Photoelastic Experiment Hybrid Method to the Fracture Mechanics of Isotropic Material, *Trans. Korea Soc. Mech. Eng. (Series A)*, **22**, 834-842.

Jai Sug Hawong, Dong Chul Shin, Hyo Jae Lee (2001), Photoelastic Experimental Hybrid Method for Fracture Mechanics of Anisotropic Material, *Experimental Mechanics*, **41**, 92-99.

D. C. Shin, J. H. Nam and D. W. Kim (2016), Experimental Interior Stress Fields of a Constantly Squeezed O-Ring Modeling from Hybrid Transmission Photoelasticity, Experimental Techniques, **40**, 59-72.

R. C. Sampson (1970), A Stress-Optic Law for Photoelastic Analysis of Orthotropic Composites, *Experimental Mechanics*, **10**, 210-215.